



Acetabular margin changes in feline hip joints – Implications for radiologic diagnosis and development of osteoarthritis

Cecilia Ley^{a,*}, Gabriela Ramer^a, Alexandra Leijon^{a,1}, Charles J. Ley^b

^a Department of Biomedical Sciences and Veterinary Public Health, Swedish University of Agricultural Sciences, SE-750 07 Uppsala, Sweden

^b Department of Clinical Sciences, Swedish University of Agricultural Sciences, SE-750 07 Uppsala, Sweden

ARTICLE INFO

Keywords:

Acetabulum
Cat
Computed tomography
Hip
OA
Osteophytes

ABSTRACT

The development and early morphological features of feline hip osteoarthritis (OA) are largely unknown. Tears in the acetabular labrum and at the chondrolabral transition zone are suggested to be important in the pathogenesis of human hip OA, but in cats such lesions have not been described. We investigated associations between computed tomography (CT)-detected joint changes and microscopic articular cartilage lesions, the distribution of detected changes, and histologically evaluated the acetabular margin (AM) in hip joints from 20 cats. Histologic evaluation was undertaken on at least one joint from each cat. CT-detected joint changes and articular cartilage lesions were graded and the histological appearance of CT-detected osteophytes evaluated. The majority of CT-detected lesions and cartilage lesions were mild. Whole-joint CT scores and AM osteophyte CT scores showed moderate to strong correlation with cartilage scores. The odds were higher for presence of CT-detected osteophytes in craniodorsal, cranial, cranioventral, ventral and dorsal AM regions. Peripheral acetabular regions showed higher cartilage lesion grades than central regions. Tears, seen as fissures/clefts, in labral and perilabral tissues were common. CT-detected AM osteophytes morphologically presented as pointed sclerotic bone, spur-shaped bone or rounded chondro-osteophytes. The results suggest that CT is a valuable tool for diagnosing early feline hip OA. CT-detected osteophytes showed variable histologic morphologies, which may implicate different disease mechanisms and/or disease stages. Tears in the AM could represent an early event in feline hip OA and this warrants further investigation.

1. Introduction

Osteoarthritis (OA) is a multifactorial joint disease characterized by destruction of articular cartilage, subchondral bone changes, osteophyte formation and variable synovitis (Chen et al., 2017; Loeser et al., 2012; Wei and Bai, 2016). Radiologically, the domestic cat suffers a high prevalence of OA (Lascelles et al., 2010; Slingerland et al., 2011) and the coxofemoral (hip) joint is commonly affected (Clarke and Bennett, 2006; Clarke et al., 2005; Freire et al., 2011; Godfrey, 2005; Lascelles et al., 2010). Studies of feline hip OA where the radiological OA diagnosis has been confirmed by pathologic examination are few (Freire et al., 2011; Kamishina et al., 2006), and none include detailed studies focused on joint margin changes and early (i.e. microscopic) evidence of cartilage degeneration in comparison to imaging findings. Studies including histologic tissue evaluation are not only important for verification of detected radiological changes as being truly OA-related, but also

valuable when attempting to establish the earliest imaging features, enabling early OA diagnosis. Additionally, identification of early imaging features of feline OA is of high importance if disease-modifying OA drugs are to be developed for cats and could be of translational value for human OA.

The feline acetabulum comprises the articulating *facies lunata* and the non-articulating *fossa acetabuli* (Liebich et al., 2007). The lunata surface is peripherally enlarged by the fibrocartilaginous *labrum acetabulare* (Liebich et al., 2007). Injuries to the acetabular labrum and the chondrolabral transition zone, located at the acetabular margin (AM), have gained considerable attention in human orthopaedics in relation to femoroacetabular impingement and a potential role in the development of hip OA (Beck et al., 2005b; Frank et al., 2015; Groh and Herrera, 2009; Hunt et al., 2007; Ito et al., 2004; Martin and Katz, 2012; McCarthy et al., 2003; McCarthy et al., 2001; Seldes et al., 2001; Su et al., 2019; Tannast et al., 2008; Tanzer and Noiseux, 2004), however

* Corresponding author.

E-mail addresses: cecilia.ley@slu.se (C. Ley), charles.ley@slu.se (C.J. Ley).

¹ A. Leijon is currently employed by AstraZeneca AB.

we are unaware of studies in cats describing histologic labral lesions.

Computed tomography (CT) is increasingly available in veterinary practice and may be a valuable tool for early OA diagnosis. CT provides cross-sectional three-dimensional (3D) images and detailed information about joint shape and morphology. CT is a powerful technique for assessing osseous features, and considering that bone is an integral component in the development of OA, the use of CT is likely to improve our understanding of the OA process (Turmezei and Poole, 2011).

We observed small spur-shaped osteophytes on the ventral AM of joints with no obvious macroscopic articular cartilage changes (Fig. S1) during initial evaluation of whole-body CT images and joint surface macroscopic evaluation of cats in an ongoing OA study. This initiated our investigations into the relevance of AM changes in feline OA. In this study, our aims were to: 1) investigate associations between CT-detected joint changes, with a focus on the AM, and microscopic articular cartilage lesions; 2) describe the distribution of detected changes; and 3) histologically evaluate features of the AM. The hypotheses were that CT-detected joint changes are associated with articular cartilage degeneration, and that the peripheral acetabular region, including the AM, represents a region for early lesion development in feline hip OA.

2. Material and methods

2.1. Study population

This observational cross-sectional exploratory study was performed post-mortem and involved the use of client-owned animals that presented for educational and research purposes at the Department of Biomedical Sciences and Veterinary Public Health, Swedish University of Agricultural Sciences (SLU). In total, 40 hip joints from 20 cats were included in the study and histologic evaluation was performed on 28 joints. Thirteen joints from seven of these cats were prospectively sampled for histology, whereas the other 15 joints from 13 cats originated from cats participating in other research studies where whole-body CT had been performed and were retrospectively evaluated. Owners' consent for their animals to participate in research was obtained for all cases as part of the submission for post-mortem examination or given in the owner consent for animal euthanasia. CT and macroscopic examinations with subsequent sampling for histology were done within one day of euthanasia, apart from two cats where the procedures were performed within two days of euthanasia.

2.2. CT examination

Whole-body CT examinations were done using a 64-slice multi-detector CT scanner (Definition, Siemens Medical Systems, Erlangen, Germany) using the settings; 250 kV, 160 mAs, slice thickness 0.6 mm, slice increment 0.3 mm and a high-resolution kernel (B70s). Cats were placed on a conforming foam cushion in ventral recumbency with the extremities extended and the head towards the gantry.

2.3. Evaluation of joint changes in CT images

Anonymized CT images were individually graded by two readers (CJL and GR) in random order using Digital Imaging and Communications in Medicine viewing software (OsiriX v 4.1.2, Pixmeo) with multiplanar reconstruction (MPR) in a bone window (window level 700 HU and window width 4000 HU). The MPR images were aligned and orientated in the same way for each cat using a standardized image orientation method (Fig. S2 and S3). The acetabulum was anatomically divided into eight, and the femoral head into five CT regions (Fig. 1). In each of these 13 regions the following lesion types were assessed: osteophytes (including enthesophytes), sclerosis, and lysis (including cyst-like lesions and subchondral bone and joint margin defects). Joint-associated (intra-/extra-articular) mineralizations were localized to the nearest acetabular region (eight regions). Lesions were graded 0 =

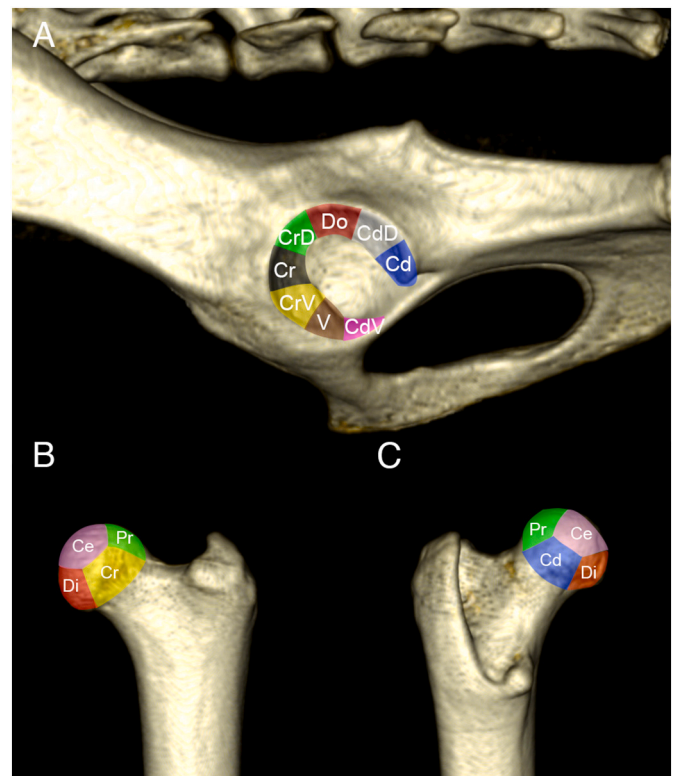


Fig. 1. Three-dimensional volumetric computed tomography (CT) images showing a lateral view of the left acetabulum (A), and cranial (B) and caudal (C) views of the left femur. Colors show regions used to localize lesions detected in CT images and histologically. For the acetabulum: CdV = caudoventral (pink); V = ventral (brown); CrV = cranioventral (yellow); Cr = cranial (black); CrD = craniodorsal (green); Do = dorsal (red); CdD = caudodorsal (grey); Cd = caudal (blue). For the femur: Ce = central (pink); Cr = cranial (yellow); Di = distal (red); Pr = proximal (green); Cd = caudal (blue). (For interpretation of the references to colour in this figure legend, the reader is referred to the web version of this article.)

normal, 1 = suspected, 2 = mild, and 3 = moderate to severe (Table S1). The highest grade of each lesion type from each region were summed to give a whole-joint CT score (CTS, maximum possible score 141 including grading of osteophytes, sclerosis and lysis in 13 regions and joint-associated mineralizations in eight regions). In a second step, one image evaluator (CJL) identified the highest grade of joint margin osteophyte in each of the eight acetabular regions and these were summed to give a AM osteophyte CT score (AMO-CTS, maximum score 24). In addition, this evaluator identified presence of spur-shaped osteophytes in the ventral region (Fig. S1).

2.4. Macroscopic examination and tissue sampling for histology

Following CT examination, the hip joints were opened and intra-articular macroscopic abnormalities recorded. Joints were graded as OA positive if cartilage lesions, including dull, yellow discolored cartilage and/or cartilage erosion/ulceration, were clearly detected; otherwise they were graded as OA negative. One or both hip joints were then removed by cutting through the body of the ilium, the ischium, the pubis, and the proximal metaphysis of the femur. The joints were fixed in 10% neutral buffered formalin and decalcified in formic acid (Kristensens lösning för urkalkning, Solveco, Rosersberg, Sweden). Following decalcification, osteochondral tissues from the articular surfaces of the acetabulum and the femur were sampled for histology. In 20/28 joints the CT images were used to guide histologic sampling with the aim of maximizing the chance of including CT-detected joint margin changes,

particularly osteophytes, in the trimmed tissue samples. In cases that did not show changes in the CT images or in non-CT-guided samples, tissue was sampled according to presence of abnormalities detected macroscopically. If no changes were detected, sampling aimed to provide the maximum articular surface for evaluation. From each joint a minimum of one sample from the acetabulum and one from the femur was obtained. In an attempt to include CT-detected joint margin changes multiple sites were sampled in 4 joints (3 joints with 2 samples from the acetabulum and 1 joint with 3 samples from the acetabulum). Samples were routinely processed and embedded in paraffin wax for light microscopic examination, cut in approximately 4 μm sections and stained with hematoxylin and eosin, and toluidine blue. Sections used for figures were photographed using a Nikon E600 light microscope and a Nikon DXM 1200 camera (Nikon Instruments, Melville, NY, USA). Light and colour adjustments were done in Adobe Photoshop version 21.1.3.

2.5. Histologic evaluation of articular cartilage and the AM

Lesions in the articular cartilage were graded according to a protocol based on the grading system by Pritzker et al. (2006) (Table S2). Grades 0–1 were considered to represent normal cartilage and the maximum lesion grade was 6.5 (Pritzker et al., 2006). Sections were coded and individually graded by two evaluators (CL and GR or CL and AL) to determine the highest lesion grade for each acetabulum and femur. When grades differed between evaluators, the final grade was decided by consensus. In a second step, four approximately equal length articular cartilage regions, two designated as peripheral (perilabral) and two as central (perifossal) were defined for the articular surfaces in each acetabular section. The femoral articular cartilage in each section was likewise divided into four approximately equally sized regions, two peripheral and two central. The location for the highest lesion grade was identified by one evaluator (CL), who subsequently also graded lesions in the other cartilage regions. In each joint, the highest lesion grade in each region of the acetabulum and femur, respectively, were summed to give an acetabular cartilage score (ACartS) (maximum score 26) and a femoral cartilage score (FCartS) (maximum score 26). A cartilage score for the whole joint (CartS) was calculated by adding the ACartS and FCartS (maximum score 52). Morphologic findings of the AM were evaluated by one of the authors (CL). Tears (fissures/clefts) were categorized in regard to location (chondrolabral transition zone vs. within *labrum acetabulare*) with reference to Seldes et al. (2001).

2.6. Determination of location of histological findings according to CT regions and evaluation of CT-detected AM osteophytes

The anonymized material was decoded. Using MPR the CT images were aligned to the histological sections. For every margin in each histological section, the corresponding CT region was determined by marking the joint margin of the section in the aligned CT and 3D volumetric reconstruction images. The histological appearance of CT-detected AM osteophytes were evaluated and described.

2.7. Statistical analyses

Descriptive analyses were performed including age, gender, breed, CTS, AMO-CTS and CartS. For analyses of effects of age on CTS, AMO-CTS and CartS cats were divided into young (0–9 years) and old (> 9 years) age groups and a Mann-Whitney *U* test was used. Spearman rank correlation was used to investigate associations between 1) CTS and CartS, 2) AMO-CTS and CartS, and 3) AMO-CTS and ACartS. Due to the uncertainty of the suspected CT-detected lesions (grade 1), the Spearman rank correlations were repeated by recalculating the CTS and AMO-CTS after exclusion of grade 1 lesions. In cats where both joints were histologically evaluated, only one joint was included in the analysis, based on choosing the joint with the highest CTS, or if the CTS were

equal, by random selection.

A logistic mixed model was used to analyse the presence/absence of CT-detected osteophytes in acetabular regions. A general linear mixed model was used to investigate differences of cartilage grades between the peripheral and central cartilage regions of the acetabulum and the femur, and residual plots checked to confirm normal distribution. Histological cartilage grades were grouped into normal (0–1), mild (1.5–2.5), moderate (3–4.5), and severe (5–6.5) for evaluation of cartilage lesion distribution and in regard to osteophyte morphology.

SigmaPlot 13.0 (Systat Software, Inc., San Jose, CA, USA) was used for descriptive, normality, Mann-Whitney *U* test and Spearman rank correlation analyses, and SAS 9.4 (SAS Institute Inc., Cary, NC, USA) was used for the mixed model analyses. *P*-values ≤ 0.05 were considered significant.

3. Results

3.1. Demographic data

The mean age was 9.9 years (median 8.5 years, range 1–19 years). Eleven cats were young (≤ 9 years) and 9 cats old (> 9 years). There were 10 neutered males, 8 neutered females and 2 intact females. Thirteen cats (65%) were Domestic Shorthaired cats and 7 cats (35%) were pure-bred (one individual each of Bengal Cat, British Shorthair, Burmese, Cornish Rex, European Shorthair, Norwegian Forest Cat, and Ragdoll).

3.2. CT-detected changes

Including both the acetabulum and the femur, osteophytes were detected in 34/40 joints (summed grades for all joints 358), sclerosis in 35/40 joints (summed grades for all joints 319), lysis in 24/40 joints (summed grades for all joints 172) and joint-associated mineralizations in 5/40 joints (summed grades for all joints 42). Lesions were more common in the acetabulum than in the femur (Fig. 2). Five joints from 3 cats were normal on CT. The CTS ($n = 20$ joints from 20 cats) ranged from 0 to 124 (mean 23.4, median 10.5), and old cats had higher CTS compared to young cats (median 25 vs. 8; $P = 0.013$).

Osteophytes were detected at the AM in 34/40 joints (17/20 cats) and at femoral margins in 15/40 joints (8/20 cats) (Fig. 2). All joints with osteophytes also showed sclerosis. The AMO-CTS ranged from 0 to 24 (mean 7.4, median 6). Older cats had higher AMO-CTS compared to younger cats (median 9 vs. 4; $P = 0.032$). The odds for the presence of AM osteophytes were significantly different between the regions ($P < 0.0001$), with craniodorsal, cranial, cranioventral, ventral and dorsal

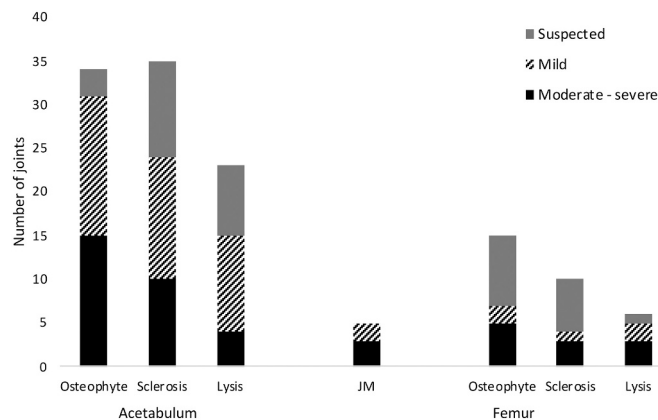


Fig. 2. Frequency and grades of lesions detected in computed tomography images ($n = 40$ joints, 20 cats). Lesions were more frequently detected in the acetabulum compared to the femur, and osteophytes and sclerosis were the most common lesion types. JM = joint-associated mineralization.

regions having higher odds compared to caudodorsal, caudal and caudoventral regions (Fig. 3).

There were 26/40 joints with osteophytes detected in the ventral AM region. Of these, 22 were spur-shaped (6 suspected, 10 small, 6 moderate to large). In 10 cats spur-shaped osteophytes were bilateral and in 2 cats they were unilateral. In all but 1 joint with ventrally located spur-shaped osteophytes, there were also osteophytes detected in other AM regions. In the 14 joints with no ventral osteophytes, 6 joints (3 cats) had no osteophytes in any other AM region and 8 joints (5 cats) had osteophytes in other AM regions.

3.3. Macroscopic appearance of articular cartilage

Macroscopic cartilage evaluation was recorded for 38/40 joints and 8 of these were macroscopically OA positive. Six of the 28 joints sampled for histology were macroscopically OA positive.

3.4. Histologic findings of articular cartilage and AM

The articular cartilage was normal or had mild changes (mean of grades given in the joint ≤ 2.5) in 23/28 joints. The CartS ranged from 0 to 49 (mean 16.4, median 14.2), ACartS from 0 to 24.5 (mean 8.5, median 6.5), and FCartS from 0 to 25.5 (mean 7.9, median 7). Old cats had higher CartS compared to young cats (median 15.5 vs. 12.5; $P = 0.01$). One cat (aged 1 year) had no microscopic cartilage lesions. Peripheral regions showed more moderate and severe lesions than central regions for both the acetabulum and the femur (Fig. 4-6) with a significant difference in lesion grades between peripheral and central regions for the acetabulum ($P = 0.0002$) but not for the femur ($P = 0.058$). The majority of lesions were mild (grades 1.5–2.5) in ventral, cranioventral, cranial, craniodorsal and dorsal acetabular regions, and in distal and cranial femoral regions. The majority of lesions were moderate or severe (grades >2.5) in caudodorsal and caudal acetabular regions and in caudal femoral regions. Caudoventral acetabular and proximal femur regions had a more even distribution of lesion grades (Fig. S4).

In total, 56 AMs were available for assessment for labral tears. In 33 AMs labral tissue was clearly detected. In 24 AMs labral tissue was continuous with the articular cartilage and in 9 AMs (7 from the ventral region) fibrous, fibrovascular or fibrocartilagenous tissue, sometimes appearing as synovium and including adipose tissue, was present between labral tissue and the articular cartilage (Fig. 7, S5 and S6). In 23 AMs the labrum was either poorly identified/absent or not possible to

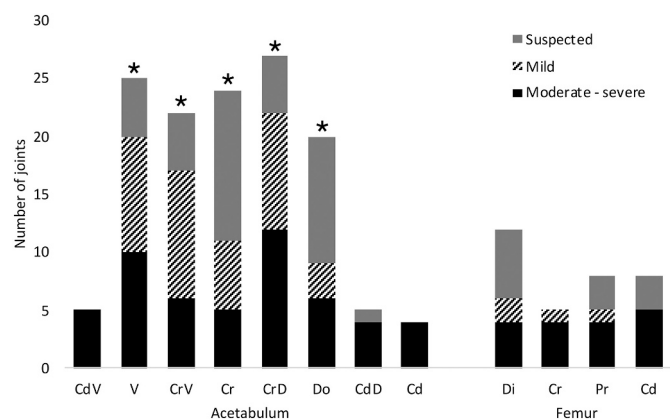


Fig. 3. Frequency and grades of osteophytes detected on the margins of the acetabulum and femur in computed tomography (CT) images ($n = 40$ joints, 20 cats). Asterisks mark regions of the acetabulum with a significantly higher frequency of osteophytes ($P < 0.0001$) compared to other acetabulum regions. CdV = caudoventral; V = ventral; CrV = cranioventral; Cr = cranial; CrD = craniodorsal; Do = dorsal; CdD = caudodorsal; Cd = caudal; Di = distal; Pr = proximal.

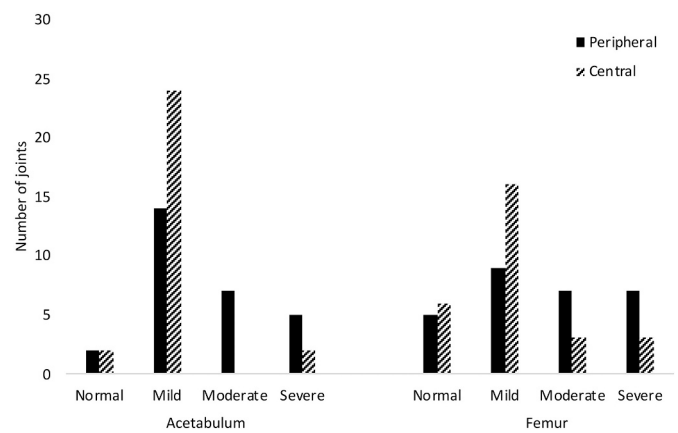


Fig. 4. Frequency of lesion grades for peripheral and central locations in the articular cartilage of the acetabulum and femur ($n = 28$ joints, 20 cats). Overall, peripheral acetabular regions showed significantly higher lesion grades compared to central acetabular regions ($P = 0.0002$).

clearly define due to artefacts or pronounced cartilage lesions or osteophytes. In assessable AMs, the labrum was detected in the cranio-dorsal region, whereas it was poorly detected/absent cranioventrally, and variably detected in the other six regions (Figs. 5, 7, 8, S5 and S6). Twelve AMs (36.4%) showed fissures/clefts of varying depth and angulation considered to be lesions. Lesions were found in both the chondrolabral transition zone and the labrum (5 AMs), in only the chondrolabral transition zone (6 AMs) or in only the labrum (1 AM) (Fig. 8). Twelve more AMs (36.4%) showed fissures/cleft-like changes that could represent normal anatomical features or processing artefacts, and thus these were not considered lesions (Fig. 7, S5 and S6).

3.5. Correlations between CT and cartilage scores

There were moderate correlations between CTS and CartS ($P = 0.0154$, $\rho = 0.533$, Fig. S7) and between AMO-CTS and CartS ($P = 0.0234$, $\rho = 0.503$, Fig. S8), and a strong correlation between AMO-CTS and ACartS ($P = 4.33 \times 10^{-6}$, $\rho = 0.749$, Fig. S9). Excluding grade 1 CT-detected lesions still showed significant correlations between CTS and CartS ($P = 0.0269$, $\rho = 0.493$), between AMO-CTS and CartS ($P = 0.0452$, $\rho = 0.451$), and between AMO-CTS and ACartS ($P = 0.0021$, $\rho = 0.646$). The one-year old cat with no detected histological cartilage lesions was normal on CT.

3.6. Histologic appearance of CT-detected AM osteophytes, associated cartilage lesions and CTS

CT-detected AM osteophytes were included in 19 microscopically examined AMs (34%). Spur-shaped bone on the AM, extending into labral tissue, corresponding to the CT-detected osteophyte was detected in 7 AMs from 7 joints (Fig. 7 and S6). These were located in ventral (5 AMs), craniodorsal (1 AM) and caudoventral (1 AM) regions. All labrae showed regions of chondroid cells, and tidemark reduplication, matrix disruption and osteoblastic-like cells lining bone cavities were variably seen (Fig. 7 and S6). Pointed sclerotic bone extending the AM corresponding to the CT-detected osteophyte was detected in 7 AMs from 7 joints (Figs. 5, 7 and 8). These were located in the cranial (3 AMs), dorsal (2 AMs), craniodorsal (1 AM) and caudodorsal (1 AM) regions. All 7 joints with with pointed sclerotic bone histologically also presented with spur-shaped osteophytes in ventral regions in CT images. Rounded osteophytes (chondro-osteophytes) corresponding to the CT-detected osteophytes were detected in 5 AMs from 3 joints (Fig. 9). These were located in dorsal, cranioventral, ventral, caudoventral and caudal regions. In joints with spur-shaped or pointed sclerotic bone no or mild articular cartilage lesions were common (present in 49/54 and 49/56

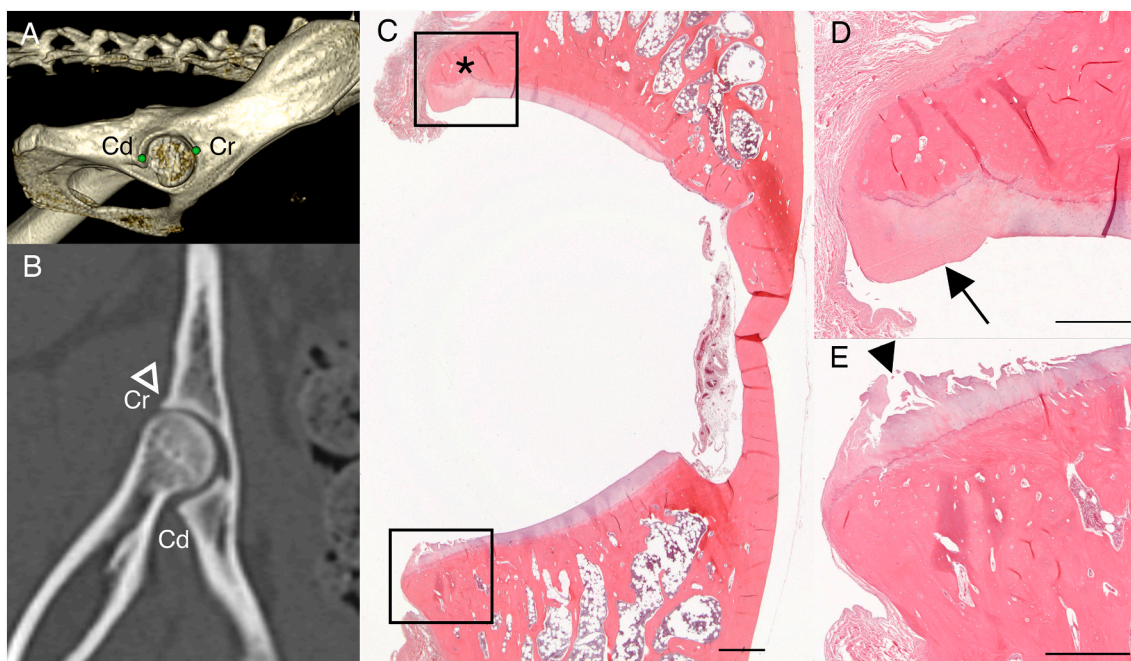


Fig. 5. Appearances of the right hip joint, 7-year-old cat. Three-dimensional reconstruction (A), and aligned computed tomography image (B) and photomicrographs (C–E) with areas within boxes magnified in (D) and (E). Green dots (A) showing the location of the cranial (Cr) and caudal (Cd) acetabular margins. A moderate cartilage lesion (grade 4) is present at the peripheral Cd margin (black arrowhead). Labral tissue is clearly defined cranially (arrow), whereas presence of labral tissue caudally cannot be assessed due to the cartilage lesion. The osteophyte located cranially (white open arrowhead) comprises pointed sclerotic bone (asterisk). Histological section stained with hematoxylin and eosin. Scale bars: (C) 1 mm, (D and E) 500 μ m. (For interpretation of the references to colour in this figure legend, the reader is referred to the web version of this article.)

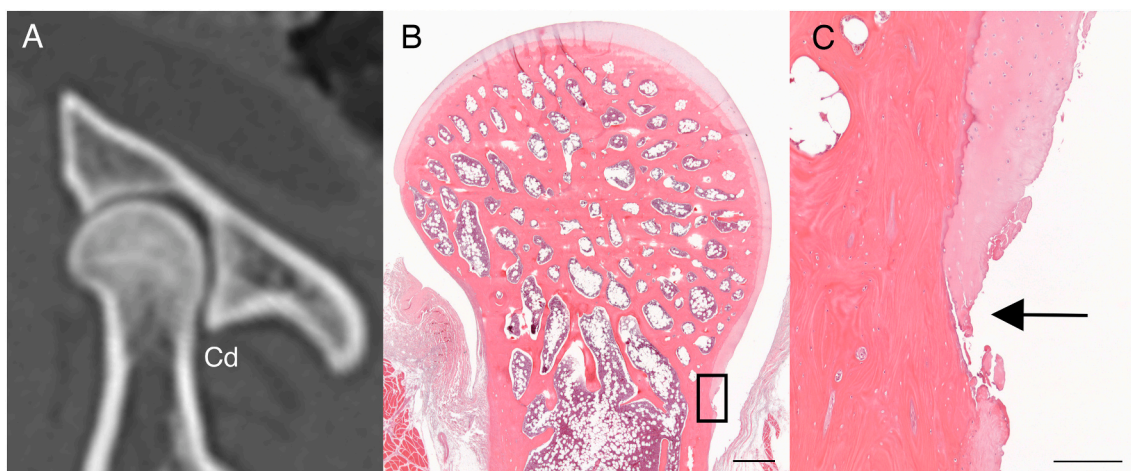


Fig. 6. Appearances of the right hip joint, 17-year-old cat. Aligned computed tomography image (A) and photomicrographs (B and C) with area within box magnified in (C). A focally severe cartilage lesion (grade 5) is present in the peripheral caudal (Cd) region of the femur (arrow) whereas other regions of the articular cartilage only show mild lesions. Histological section stained with hematoxylin and eosin. Scale bars: (B) 1 mm, (C) 200 μ m.

cartilage regions, respectively). In joints with rounded osteophytes moderate to severe cartilage lesions were common (present in 20/24 regions). The CTS ranged from 7 to 24 (mean 12, median 11) in joints with spur-shaped bone, from 9 to 34 (mean 18, median 16) in joints with pointed sclerotic bone, and from 44 to 124 (mean 92.7, median 110) in joints with rounded osteophytes. Macroscopically, all 3 joints with rounded osteophytes were OA positive, but only 1 joint with a spur-shaped hook and 1 joint with pointed sclerotic bone were macroscopically OA positive.

4. Discussion

In this study we evaluated CT-detected joint changes associated with the presence of cartilage lesions in feline hip joints, with a specific focus on AM osteophytes. We described the distribution of detected lesions, the morphology of CT-detected osteophytes and evaluated presence of microscopic tears at the chondrolabral transition zone and the acetabular labrum. To our knowledge, no studies in cats have previously evaluated CT-detected changes compared to cartilage lesions or evaluated microscopic AM changes, although the use of CT for quantitative morphometric measurements in a single case of hip dysplasia has been reported (Lai et al., 2016).

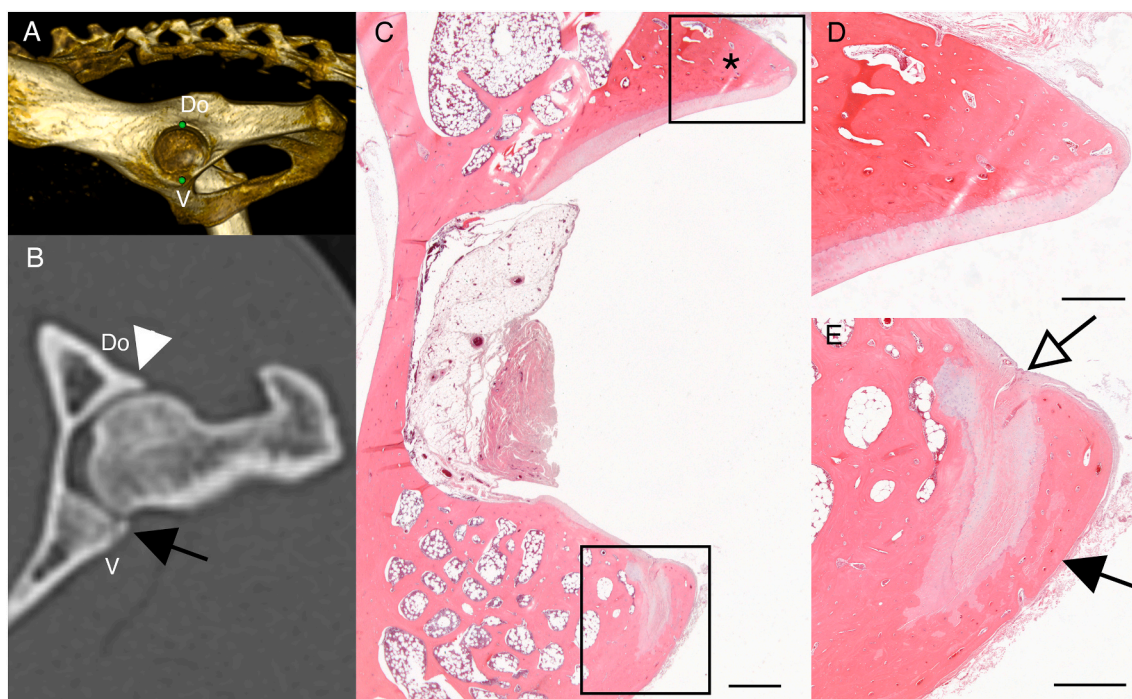


Fig. 7. Appearances of the left hip joint, 6-year-old cat. Three-dimensional reconstruction (A), and aligned computed tomography image (B) and photomicrographs (C–E), with areas within boxes magnified in (D) and (E). Green dots (A) showing the location of the dorsal (Do) and ventral (V) acetabular margins. The dorsally located osteophyte (white arrowhead) comprises pointed sclerotic bone (asterisk), whereas the ventrally located osteophyte comprises spur-shaped bone in labral tissue (black arrows). A fissure-like change is present in fibrovascular tissue located between the articular cartilage and the labrum (open arrow). Labral tissue is absent dorsally. Histological section stained with hematoxylin and eosin. Scale bars: (C) 1 mm, (D and E) 500 μ m. (For interpretation of the references to colour in this figure legend, the reader is referred to the web version of this article.)

CTS and CartS were moderately correlated and were both higher in old cats compared to young cats. This is in accordance with the age-associated increase of OA previously shown for cats (Freire et al., 2014; Ryan et al., 2013; Slingerland et al., 2011), and the increase in severity of cartilage lesions with age reported for the feline stifle joint (Leijon et al., 2017). This finding supports the hypothesis that the evaluated parameters are representative of OA and that CT is a valuable tool for diagnosing feline hip OA. Lack of macroscopic cartilage lesions together with presence of mild histologic cartilage lesions in most joints further suggests that bone changes develop early in the OA disease process and that CT is useful when evaluating the early stages of the disease (i.e. before macroscopic cartilage lesions are detected).

A strong correlation between AMO-CTS and ACartS, and a moderate correlation between AMO-CTS and CartS suggest that osteophytes on the AM are an important radiological sign of feline hip OA. This finding agrees with previous imaging studies in cats (Freire et al., 2011; Guillot et al., 2012). In the present study the numbers of joints with osteophytes and sclerosis were approximately equal. This is in contrast to a previous feline study where digital radiography was used and osteophytes were detected in 86% and sclerosis in 10% of hip joints (Freire et al., 2011). The high number of joints with sclerosis in the present study may relate to the assumption that CT is more sensitive for detection of sclerosis than radiography (Turmezei and Poole, 2011). However, the total sum of grades for osteophytes was higher than the sum for sclerosis, which suggests that osteophytes are more common than sclerosis in feline hip OA. In human knee OA, marginal osteophytes were reported to be the most sensitive radiographic finding, whereas sclerosis was an insensitive radiographic sign of OA and rarely detected in absence of associated osteophytes (Kijowski et al., 2006).

Although few joints showed evidence of cartilage degeneration macroscopically, microscopic cartilage lesions were common. Discrepancy between numbers of joints with macroscopic and microscopic OA has previously been described for feline elbow joints (Freire et al.,

2014), and the low number of macroscopically detected lesions in the present study is likely related to most histological lesions being mild. Microscopic cartilage lesion grades were significantly higher in peripheral compared to central (perifossal) locations of the acetabulum and there was a trend towards higher lesion grades in peripheral locations for the femur. This suggests that the peripheral part of the joint represents the earliest site for cartilage lesions to develop in feline hip OA.

Microscopic cartilage lesions were detected in all CT-specified regions of the acetabulum and the femur. Due to the study design it is not possible to draw firm conclusions from the cartilage lesion severity in regard to regions, and the seemingly more severe lesions in caudodorsal and caudal acetabular regions and in caudal femoral regions need to be cautiously interpreted. Most joints were sampled in specifically selected regions guided by CT-detected changes, an uneven number of samples were evaluated from the different regions, and the CT-guided sampling resulted in an overrepresentation of examined samples from the region opposite the selected sampling site.

Fissures/clefts were common at the chondrolabral transition zone and within the labrum. A potential role of these in the development of feline OA is to be determined. The lack of available information of normal histology of the feline labrum meant that interpretation of findings in some sections was not possible. Microscopic labral tears have been reported in as many as 96% of aging human hips (Seldes et al., 2001). Studies have shown that chondral lesions are common in joints with labral fraying or tears, and that in the vast majority the cartilage damage occurs in the same acetabular region as the labral lesion (McCarthy et al., 2001). It has also been speculated that labral tears are involved in the development of peripheral osteophytes (Seldes et al., 2001). Causes of labral tears in people include traumatic injury, femoroacetabular impingement, capsular laxity/joint hypermobility, dysplasia and degeneration (Groh and Herrera, 2009). In the present study etiologic factors were not investigated. However, it is possible that

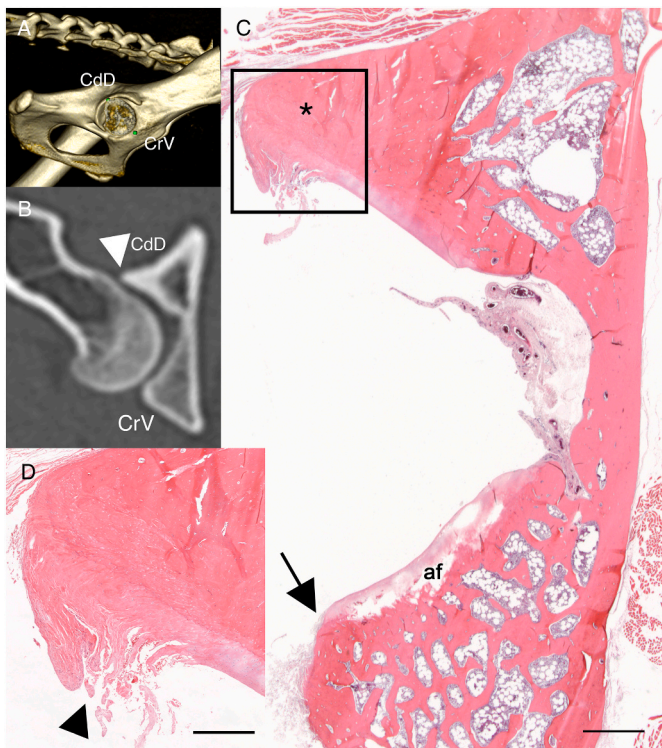


Fig. 8. Appearances of the right hip joint, 7-year-old cat. Three-dimensional reconstruction (A), and aligned computed tomography image (B), and photomicrographs (C and D), with area within box magnified in (D). Green dots (A) showing the location of the caudodorsal (CdD) and cranioventral (CrV) acetabular margins. Fissures (black arrowhead) are present both at the chondrolabral transition zone and in the labrum caudodorsally. Labral tissue is absent cranioventrally (black arrow). The osteophyte caudodorsally (white arrowhead) comprises pointed sclerotic bone (asterisk). Tissue loss representing sectioning artefacts are present cranioventrally (af). Histological sections stained with hematoxylin and eosin. Scale bars: (D) 500 μ m, (C) 1 mm. (For interpretation of the references to colour in this figure legend, the reader is referred to the web version of this article.)

joints exhibiting acetabular conformation with prominent pointed sclerotic bone at the AM could represent pincer-like morphology, since this is characterized by osseous tissue extending over the normal acetabular rim (Röling et al., 2020; Su et al., 2019), and studies focusing on the conformation of feline hips may be valuable for increased understanding of the pathogenesis of feline hip OA.

In the ventral acetabular region fibrous/fibrovascular tissue were detected peripheral to the articular cartilage. Since this also was found in the normal one-year old cat and cartilage lesion scores in affected joints typically were low we suspect that the finding is not a true lesion. It may be similar to the fibrocellular surface tissue described at the chondrolabral transition zone and the capital parafoveal area in human hip joints, considered a non-progressive change (Byers et al., 1976).

Osteophytes were more frequently detected with CT on the AM than the femoral head/neck, which is in agreement with other studies (Keller et al., 1999). The most common locations of CT-detected osteophytes were cranial, craniodorsal, dorsal, cranioventral and ventral AM regions. This agrees with a study of feline hip dysplasia, where the craniodorsal AM was the most common location for degenerative changes to be detected radiographically (Keller et al., 1999). A feline in vitro model showed that the load distribution from the femur at mid stance mainly involves the acetabular regions corresponding to the craniodorsal, dorsal, caudodorsal and caudal CT regions in our study (Beck et al., 2005a), which could explain why CT-detected osteophytes showed sclerotic bone in cranial, craniodorsal and dorsal regions.

Microscopic examination of CT-detected AM osteophytes revealed a variety of morphologies; spur-shaped bone, pointed sclerotic bone and rounded osteophytes. It is possible that the variable morphologies are associated with different processes or represent different developmental stages of OA. These findings highlight the importance of histopathology for increased understanding of the pathogenesis of OA. Joints with rounded osteophytes showed a high degree of moderate to severe cartilage lesions and high CTS (indicating involvement of the entire joint) and can be considered to represent advanced OA (Pritzker et al., 2006). Due to the common finding of predominately mild cartilage lesions in joints with spur-shaped and pointed sclerotic bone these morphologies may be a sign of early OA. CT-detected ventrally located spur-shaped osteophytes typically concurred with osteophytes in other joint regions and it can be speculated that they are associated with OA. Alternatively, the spur-shaped bone could represent adaption to loading of the labrum or a primary labral disease process that may initiate OA. To the authors' knowledge, spur-shaped osteophytes located in the ventral AM region have not previously been reported in cats. These spurs are not expected to be visible in standard ventrodorsal and lateral radiographs of feline hip joints due this region being summated on the pelvis. It is unclear how common ventral spurs are in the general cat population and to investigate how they progress with advancing OA requires longitudinal studies.

There are several limitations to take into consideration in this study, one being the relatively small number of animals included. Another limitation is that although there appeared to be regional patterns for the different morphologic osteophyte appearances, the results can only be related to the specific locations examined histologically, and the true extent of the morphological distribution was not histologically verified. Furthermore, it would have been optimal to examine the entire articular surface for presence of microscopic lesions as lesions of other grades or in other locations could have been present in non-examined tissue. However, this was not possible with the techniques used. Plain CT images do not provide detailed information about the articular cartilage and the acetabular labrum since it is not possible to define cartilage from the synovial fluid and soft tissues. Despite this, the findings in the current study show that osteophytes on the AM detected in CT images reflect histological changes in the articular cartilage. Articular cartilage and labral lesions can be detected with positive arthrography in human hip joints (Henak et al., 2014). However, this technique has not been developed in cats and injections into the feline hip joint are challenging (Clements, 2006). Contrast-enhanced CT methods for estimating the proteoglycan content of the articular cartilage, which reflect the early/mild stages of OA, have been described in humans and animal species other than the cat (Bhattarai et al., 2020; Kokkonen et al., 2014; Lakin et al., 2017). However, due to the very thin feline articular cartilage these methods are unlikely to be useful in cats using clinical CT equipment and were not attempted in the study. Magnetic resonance imaging can provide whole-joint assessment of articular cartilage, however a high-field (4.7 Tesla) magnetic resonance imaging study with comparison to macroscopy and histology reported that due to the thin articular cartilage in cats and the resolution limitations of this method, magnetic resonance imaging only provides limited information about mild cartilage lesions in cats (Kamishina et al., 2006).

The lack of information in the literature about the CT appearance of the feline hip means that the CT grading was exploratory and based on previously described radiographical changes associated with feline OA (Freire et al., 2011; Lascelles et al., 2010). The CT scores were correlated to microscopic cartilage lesions and this supports the validity of the CT grading. In the CT grading a grade 1 represented a suspected mild lesion, with definite lesions being grade 2 or 3. When suspected lesions were removed from the data set significant correlations between CT lesions and articular cartilage scores remained. The correlation coefficients were mildly lower when the suspected lesions were excluded, suggesting that the suspected CT lesions were associated with cartilage lesions.

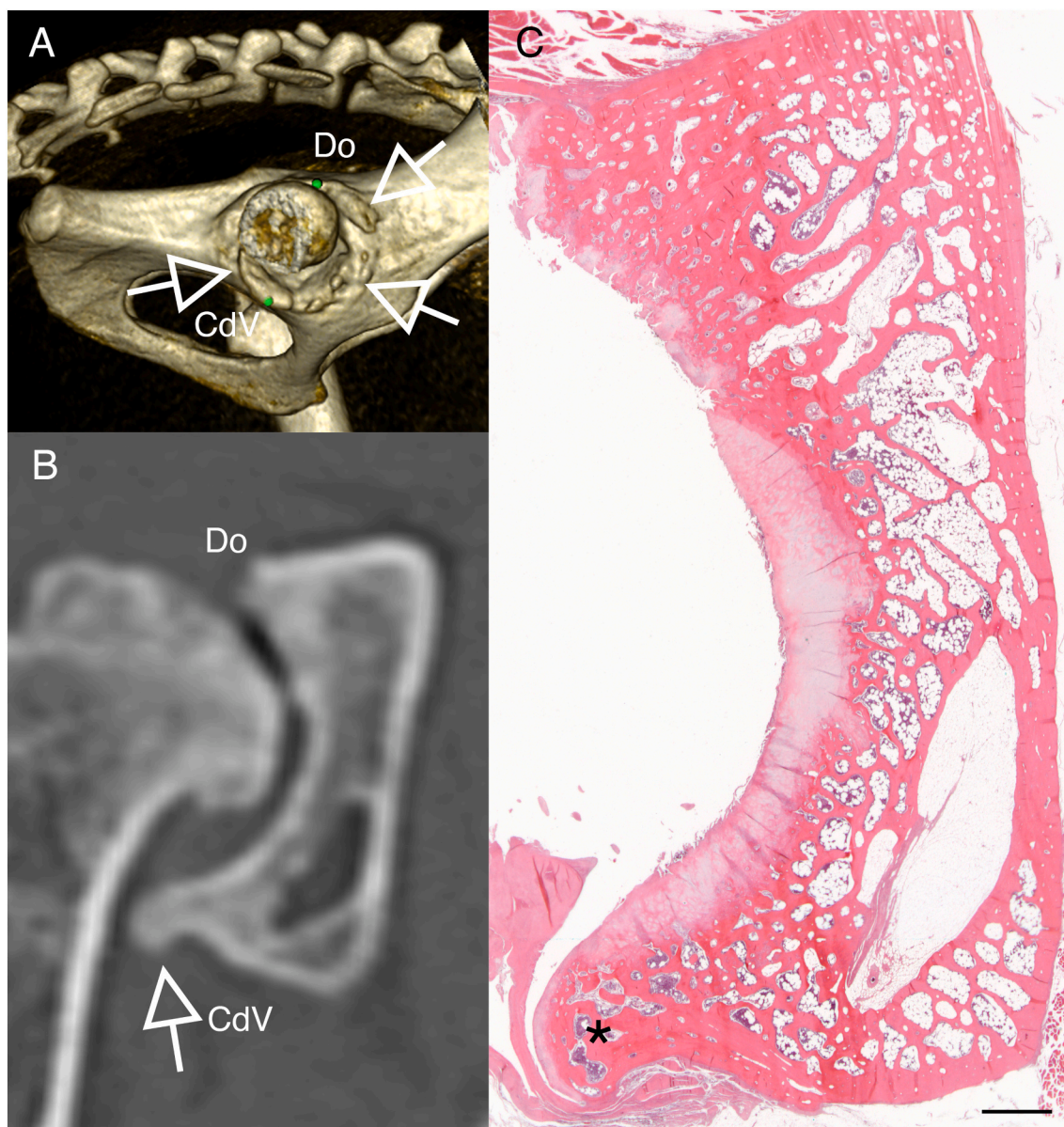


Fig. 9. Appearances of the right hip joint, 11-year-old cat. Three-dimensional reconstruction (A), and aligned computed tomography image (B) and two joined photomicrographs (C). Green dots (A) showing the location of the dorsal (Do) and caudoventral (CdV) acetabular margins. In computed tomography images large osteophytes (open arrows) are seen around the acetabular margins (A and B), as well as severe remodeling of the acetabulum and femoral head shape and subchondral sclerosis of the femoral head and dorsal aspect of the acetabulum (B). The large osteophyte located caudoventrally (open arrow in B) comprises a rounded chondro-osteophyte (asterisk). Moderate to severe cartilage lesions with grades ranging from 3.5–6.5 (C). Histological section stained with hematoxylin and eosin. Scale bar: (C) 1 mm. (For interpretation of the references to colour in this figure legend, the reader is referred to the web version of this article.)

5. Conclusions

The results of this study suggest that CT is a valuable tool for diagnosing feline hip OA and has good potential for diagnosing OA at an early stage. CT-detected AM osteophytes show several different histologic morphologies, which may implicate different disease mechanisms and/or stages in the development of OA. Ventrally located spur-shaped osteophytes within the labrum may be part of early OA or represent a primary labral disease. The results indicate that the perilabral cartilage is an area sensitive to cartilage degradation. Similar to discussed in humans, lesions in the acetabular labrum and the chondrolabral transition zone may be important in the development of feline hip OA.

Supplementary data to this article can be found online at <https://doi.org/10.1016/j.rvsc.2021.05.010>.

Declaration of Competing Interest

None.

Acknowledgements

This study was supported by SLU, Djurvännernas förening in Stockholm, and Agria and Swedish Kennel Club Research Fund (Agria och Svenska Kennelklubben Forskningsfond, grant number N2013-007). The authors thank the SLU co-workers; Vidar Skullerud, Albin Norman, Christina Nilsson, Agneta Boström and Peder Eriksson, Department of Biomedical Sciences and Veterinary Public Health, for technical assistance and Claudia von Brömmesen, Department of Energy and Technology, for statistical assistance.

References

- Beck, A.L., Pead, M.J., Draper, E., 2005a. Regional load bearing of the feline acetabulum. *J. Biomech.* 38, 427–432.
- Beck, M., Kallhor, M., Leunig, M., Ganz, R., 2005b. Hip morphology influences the pattern of damage to the acetabular cartilage: femoroacetabular impingement as a cause of early osteoarthritis of the hip. *J. Bone Joint Surg. (Br.)* 87, 1012–1018.
- Bhattacharai, A., Pouran, B., Mäkelä, J.T.A., Shaikh, R., Honkanen, M.K.M., Prakash, M., Kröger, H., Grinstaff, M.W., Weinans, H., Jurvelin, J.S., Töyräs, J., 2020. Dual contrast in computed tomography allows earlier characterization of articular cartilage over single contrast. *J. Orthop. Res.* 38, 2230–2238.
- Byers, P.D., Contepomi, C.A., Farkas, T.A., 1976. Post-mortem study of the hip joint. II. Histological basis for limited and progressive cartilage alterations. *Ann. Rheum. Dis.* 35, 114–121.
- Chen, D., Shen, J., Zhao, W., Wang, T., Han, L., Hamilton, J.L., Im, H.J., 2017. Osteoarthritis: toward a comprehensive understanding of pathological mechanism. *Bone Res.* 5, 16044.
- Clarke, S.P., Bennett, D., 2006. Feline osteoarthritis: a prospective study of 28 cases. *J. Small Anim. Pract.* 47, 439–445.
- Clarke, S.P., Mellor, D., Clements, D.N., Gemmill, T., Farrell, M., Carmichael, S., Bennett, D., 2005. Prevalence of radiographic signs of degenerative joint disease in a hospital population of cats. *Vet. Rec.* 157, 793–799.
- Clements, D., 2006. Arthrocentesis and synovial fluid analysis in dogs and cats. In *Practice* 28, 256–262.
- Frank, J.M., Harris, J.D., Erickson, B.J., Slikker 3rd, W., Bush-Joseph, C.A., Salata, M.J., Nho, S.J., 2015. Prevalence of femoroacetabular impingement imaging findings in asymptomatic volunteers: a systematic review. *Arthroscopy* 31, 1199–1204.
- Freire, M., Robertson, I., Bondell, H.D., Brown, J., Hash, J., Pease, A.P., Lascelles, B.D., 2011. Radiographic evaluation of feline appendicular degenerative joint disease vs. macroscopic appearance of articular cartilage. *Vet. Radiol. Ultrasound* 52, 239–247.
- Freire, M., Meuten, D., Lascelles, D., 2014. Pathology of articular cartilage and synovial membrane from elbow joints with and without degenerative joint disease in domestic cats. *Vet. Pathol.* 51, 968–978.
- Godfrey, D.R., 2005. Osteoarthritis in cats: a retrospective radiological study. *J. Small Anim. Pract.* 46, 425–429.
- Groh, M.M., Herrera, J., 2009. A comprehensive review of hip labral tears. *Curr. Rev. Musculoskelet. Med.* 2, 105–117.
- Guillot, M., Moreau, M., d'Anjou, M.A., Martel-Pelletier, J., Pelletier, J.P., Troncy, E., 2012. Evaluation of osteoarthritis in cats: novel information from a pilot study. *Vet. Surg.* 41, 328–335.
- Henak, C.R., Abraham, C.L., Peters, C.L., Sanders, R.K., Weiss, J.A., Anderson, A.E., 2014. Computed tomography arthrography with traction in the human hip for three-dimensional reconstruction of cartilage and the acetabular labrum. *Clin. Radiol.* 69, e381–e391.
- Hunt, D., Clohisy, J., Prather, H., 2007. Acetabular labral tears of the hip in women. *Phys. Med. Rehabil. Clin. N. Am.* 18 (497–520), ix–x.
- Ito, K., Leunig, M., Ganz, R., 2004. Histopathologic features of the acetabular labrum in femoroacetabular impingement. *Clin. Orthop. Relat. Res.* 262–271.
- Kamishina, H., Miyabayashi, T., Clemmons, R.M., Farese, J.P., Uhl, E.W., Silver, X., 2006. High field (4.7 T) magnetic resonance imaging of feline hip joints. *J. Vet. Med. Sci.* 68, 285–288.
- Keller, G.G., Reed, A.L., Lattimer, J.C., Corley, E.A., 1999. Hip dysplasia: a feline population study. *Vet. Radiol. Ultrasound* 40, 460–464.
- Kijowski, R., Blankenbaker, D., Stanton, P., Fine, J., De Smet, A., 2006. Correlation between radiographic findings of osteoarthritis and arthroscopic findings of articular cartilage degeneration within the patellofemoral joint. *Skelet. Radiol.* 35, 895–902.
- Kokkonen, H.T., Suomalainen, J.S., Joukainen, A., Kröger, H., Sirola, J., Jurvelin, J.S., Salo, J., Töyräs, J., 2014. In vivo diagnostics of human knee cartilage lesions using delayed CBCT arthrography. *J. Orthop. Res.* 32, 403–412.
- Lai, A., Culvenor, J., Bailey, C., 2016. Morphometric assessment of hip dysplasia in a cat treated by juvenile pubic symphysiodesis. *Vet. Comp. Orthop. Traumatol.* 29, 433–438.
- Lakin, B.A., Snyder, B.D., Grinstaff, M.W., 2017. Assessing cartilage biomechanical properties: techniques for evaluating the functional performance of cartilage in health and disease. *Annu. Rev. Biomed. Eng.* 19, 27–55.
- Lascelles, B.D., Henry 3rd, J.B., Brown, J., Robertson, I., Sumrell, A.T., Simpson, W., Wheeler, S., Hansen, B.D., Zamprogno, H., Freire, M., Pease, A., 2010. Cross-sectional study of the prevalence of radiographic degenerative joint disease in domesticated cats. *Vet. Surg.* 39, 535–544.
- Leijon, A., Ley, C.J., Corin, A., Ley, C., 2017. Cartilage lesions in feline stifle joints - associations with articular mineralizations and implications for osteoarthritis. *Res. Vet. Sci.* 114, 186–193.
- Liebich, H.-G., König, H.E., Maierl, J., 2007. In: König, H.E., Liebich, H.-G. (Eds.), *Veterinary Anatomy of Domestic Animals*, 3rd ed. Schattauer, Stuttgart, Germany, pp. 215–276.
- Loeser, R.F., Goldring, S.R., Scanzello, C.R., Goldring, M.B., 2012. Osteoarthritis: a disease of the joint as an organ. *Arthritis Rheum.* 64, 1697–1707.
- Martin, S.D., Katz, N., 2012. Labral tears and femoroacetabular impingement: clinical features and arthroscopic management. *Open Arthritis J.* 5, 1–13.
- McCarthy, J.C., Noble, P.C., Schuck, M.R., Wright, J., Lee, J., 2001. The Otto E. Aufranc Award: the role of labral lesions to development of early degenerative hip disease. *Clin. Orthop. Relat. Res.* 25–37.
- McCarthy, J., Noble, P., Aluisio, F.V., Schuck, M., Wright, J., Lee, J.A., 2003. Anatomy, pathologic features, and treatment of acetabular labral tears. *Clin. Orthop. Relat. Res.* 38–47.
- Pritzker, K.P., Gay, S., Jimenez, S.A., Ostergaard, K., Pelletier, J.P., Revell, P.A., Salter, D., van den Berg, W.B., 2006. Osteoarthritis cartilage histopathology: grading and staging. *Osteoarthr. Cartil.* 14, 13–29.
- Röling, M.A., Mathijssen, N.M.C., Bloem, R.M., 2020. Diagnostic sensitivity and specificity of dynamic three-dimensional CT analysis in detection of cam and pincer type femoroacetabular impingement. *BMC Musculoskelet. Disord.* 21, 37.
- Ryan, J.M., Lascelles, B.D., Benito, J., Hash, J., Smith, S.H., Bennett, D., Argyle, D.J., Clements, D.N., 2013. Histological and molecular characterisation of feline humeral condylar osteoarthritis. *BMC Vet. Res.* 9, 110.
- Seldes, R.M., Tan, V., Hunt, J., Katz, M., Winiarsky, R., Fitzgerald Jr., R.H., 2001. Anatomy, histologic features, and vascularity of the adult acetabular labrum. *Clin. Orthop. Relat. Res.* 232–240.
- Slingerland, L.I., Hazewinkel, H.A., Meij, B.P., Picavet, P., Voorhout, G., 2011. Cross-sectional study of the prevalence and clinical features of osteoarthritis in 100 cats. *Vet. J.* 187, 304–309.
- Su, T., Chen, G.X., Yang, L., 2019. Diagnosis and treatment of labral tear. *Chin. Med. J.* 132, 211–219.
- Tannast, M., Goricki, D., Beck, M., Murphy, S.B., Siebenrock, K.A., 2008. Hip damage occurs at the zone of femoroacetabular impingement. *Clin. Orthop. Relat. Res.* 466, 273–280.
- Tanzer, M., Noiseux, N., 2004. Osseous abnormalities and early osteoarthritis. The role of hip impingement. *Clin. Orthop. Relat. Res.* 429, 170–177.
- Turmezei, T.D., Poole, K.E., 2011. Computed tomography of subchondral bone and osteophytes in hip osteoarthritis: the shape of things to come? *Front. Endocrinol. (Lausanne)* 2, 97.
- Wei, Y., Bai, L., 2016. Recent advances in the understanding of molecular mechanisms of cartilage degeneration, synovitis and subchondral bone changes in osteoarthritis. *Connect. Tissue Res.* 57, 245–261.